ELSEVIER

International Journal of Pharmaceutics 241 (2002) 173–184

international journal of pharmaceutics

www.elsevier.com/locate/ijpharm

Influence of teardrop studs on rotating frictional base plate on spheroid quality in rotary spheronization

P.W.S. Heng *, C.V. Liew, L. Gu

Department of Pharmacy, Faculty of Science, National University of Singapore, 18 Science Drive 4, Singapore 117543, Singapore

Received 8 June 2001; received in revised form 19 April 2002; accepted 25 April 2002

Abstract

The effects of teardrop-shaped studs on the quality of rotary processed spheroids were investigated. The spheroids were produced under similar conditions using three rotating frictional base plates with teardrop studs of different height, volume, cross-sectional area and surface area. Spheroid properties were rated by size, size distribution, shape, friability and density. The amounts of lumps and fines produced, and the adhesion of material on the rotating frictional base plates was also looked into. The dimension of the teardrop studs on the rotating frictional base plate affected spheroid quality. The resultant shear forces and energy input during rotary spheronization differed depending on the different height, volume, cross-sectional area and surface area of studs. With the increase in height, volume, cross-sectional area and surface area of studs on the frictional base plate, the mass median diameter, e_R and circularity of spheroids increased with corresponding decrease in span, lumps and fines. Although the frictional base plate with shortest studs had little adhesion, it may not supply enough shear force and energy input for the spheronization process, resulting in a less stable process. A balance between energy input and adhesion on the rotating frictional base plate was needed in order to optimize the production of spheroids by rotary processing.

Keywords: Rotary processor; Rotary processing; Teardrop studs; Frictional base plate; Spheroids

1. Introduction

The rotary processor, also referred to as a rotary fluid bed, can be used to produce spheroids from powder in a single step process (Parikh et al., 1997). The formation of spheroids by rotary processing consists basically of three stages: liquid addition, tumbling and drying. Unlike spheroid production by extrusion-spheronization, the production of rotary processed spheroids bypasses the extrusion stage. The rotating frictional base plate provides the centrifugal force which propels the spheroids towards the wall of the processing chamber and kinetic force for material movement. The material assumes a tumbling rope-like motion on the rotating frictional base plate. In the absence of specialized tools for mixing and for breaking up adhered masses, the rotary processor relies largely on the forces set up by the rotating

* Corresponding author. Tel.: +65-68742930; fax: +65-67752265.

E-mail address: phapaulh@nus.edu.sg (P.W.S. Heng).

0378-5173/02/$ - see front matter
PII: S0378-5173(02)00236-3

frictional base plate to bring about liquid distribution and mixing during the liquid addition stage.

In attempts to reduce adhesion on the rotating frictional base plate, operating conditions need to be optimized (Liew et al., 2000a). Another factor of importance is the type of protuberances on the plate. The surface of the rotating frictional base plate may be designed specially to meet specific applications. In the case of drug layering with nonpareil seeds or coating with core spheroids, plates with smooth surfaces may be used in place of those with protuberances on their surfaces. The reason is that nonpareil seeds and core spheroids generally have better flow properties than powders and are able to tumble in a rope-like motion on plates with smooth surfaces. A smooth plate is also best for avoiding material adhesion but it does not supply sufficient shear for effective spheronization. The patterned plates can supply higher shear but have a greater tendency to cause material adhesion. Plates with grooved surfaces are used in extrusion-spheronization. The edges of the grooves were required to facilitate the initial cutting up of extrudates to form shorter and almost uniform length segments. For rotary processing, a frictional base plate with protuberances on the surface was also required. However, the edges of these protuberances need not be angular as there was no cutting up of extrudates required. Thus, studs with a smooth but undulating design was desirable. The shear force provided by such studs need to be sufficient for aiding the mixing of the moist powder mass, promoting agglomeration, rounding and smoothening of agglomerates during spheroid production, and for maintaining a uniform tumbling motion of spheroids during drying without causing excessive attrition and fragmentation. Studs described as pyramidally-shaped elevations or square studs with rounded edges positioned in a cross hatched pattern on the surface of the rotating frictional base plate have been used in spheroid production by rotary processing (Liew et al., 1998, 2000a; Holm, 1996; Wan et al., 1994, 1995). Following these studies, studs were redesigned so that they provide the necessary shear force with minimal material adhesion. The objective of the current study was to assess the effect of three rotating frictional base plates with teardrop-shaped studs of different height, volume, cross-sectional area, surface area on the quality of microcrystalline cellulose: lactose spheroids.

2. Materials and methods

2.1. Materials

Spheroids were prepared from a binary mixture of lactose monohydrate (Pharmatose® 200M, De Melkindustrie Veghel, The Netherlands) and microcrystalline cellulose (MCC; Avicel PH-101, Asahi Chemical, Japan) in a ratio of 3:1. Distilled water was used as the moistening liquid.

2.2. Methods

2.2.1. Equipment

The multisystem fluidized-bed (MP-1, Aeromatic-Fielder, UK) with the rotary processor insert was used for the rotary spheronization experiments. The rotary processor was a double chamber system consisting of an inner chamber housed inside a large outer chamber. The rotating frictional base plate resided within the inner chamber, with a narrow gap between the edge of the rotating frictional base plate and the inner chamber wall. A positive air pressure was maintained at the gap to push material upwards, preventing material loss through the gap into the rotor housing below. A thin perforated metal ring encircled the circumferential area separating the two chambers. Fluidizing air can be introduced into the system via the perforations on the metal ring. The wall of the inner product chamber was lined with polytetrafluoroethylene (PTFE) tape to reduce the adhesion of wetted material to the container wall during processing (Liew et al., 1998). The inner wall was lifted during the drying stage to allow spheroids to be dried by the fluidizing air.

Three rotating frictional base plates with teardrop-shaped studs were used. The three plates, with an outer diameter of 275 mm, had the same number of studs ($n = 140$) on their surfaces. The studs were arranged in a similar pattern for

all three plates (Fig. 1). The characteristics of the studs were summarized in Table 1. The measurements of height and cross-sectional area were made with reference to the tallest part of the studs (Fig. 1). For characterizing the surface area of the stud, a flexible transparent film was used to envelope the studs forming a skin on the studs. The film was then carefully detached, edges trimmed and surface area determined using a graphic paper by spreading the film gently over the paper. The measurement was repeated for ten randomly chosen studs for each plate.

Next, impression models of the studs were made using clay by carefully fitting the clay over the studs. The weight of testing liquid required to fill each impression model was noted. The testing liquid was a 0.05% polysorbate 85 (Merck, Germany) aqueous solution. A calibration line of weight against volume of testing liquid was first plotted. The volume of the stud, i.e. the volume of testing liquid required for filling the impression model, was determined from the weight of testing liquid used and the calibration plot. The test was repeated for ten randomly chosen studs for each plate.

2.2.2. Preparation of spheroids

A total weight of 600 g of MCC and lactose in a ratio of 1:3 was dry-mixed in a 4-l laboratory double cube mixer (J. Engelsmann AG, JEL, Germany) rotating at 47.8 rpm for 30 min. The powder mix was then transferred to the rotary processor (MP-1, Aeromatic Fielder). Moistening liquid amounting to 225 ml was sprayed onto the rotating powder mix at a rate of 27 ml/min using a peristaltic pump (504U, Watson Marlow, UK). The atomizing pressure was set at 1.2 bar and a gap air pressure of 1.5 bar was used. During the liquid addition and tumbling stages, the inlet air temperature was set at 30 °C. The speed of the rotating frictional base plate was varied following a 'low-high-low' speed variation protocol (Liew et al., 2000a). The rotating frictional base plate was rotated at 100 rpm initially for 20 s, and then increased to 520 rpm and maintained for 2 min. After the powder was wetted, the frictional base

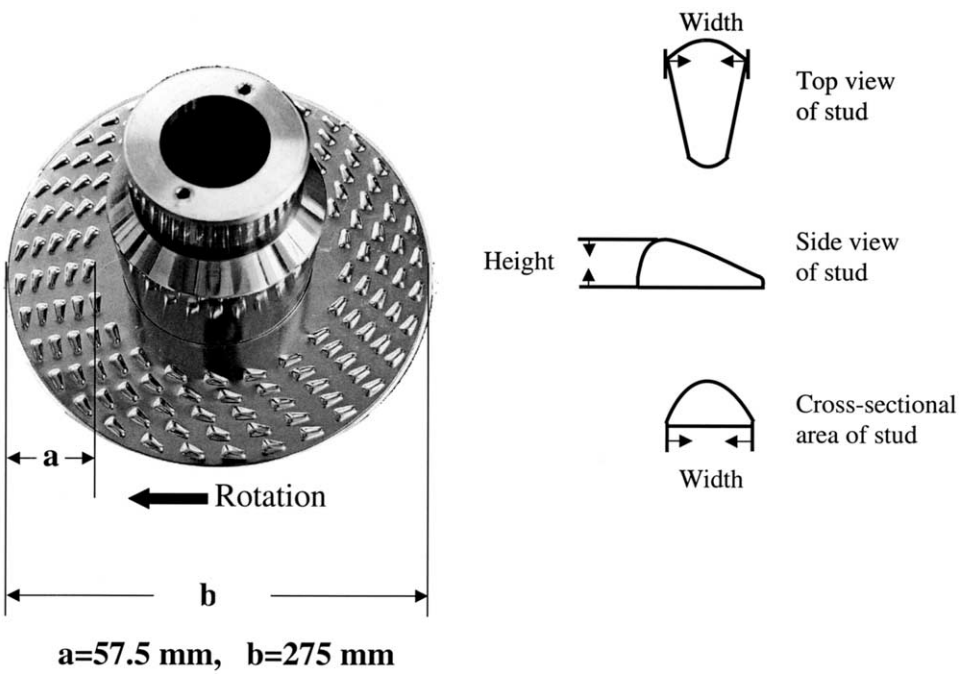

Fig. 1. Schematic diagram of frictional base plate with teardrop studs.

Table 1
Characteristics of teardrop studs on the three frictional base plates

Plate	Studs properties			
	Height (mm)	Volume (mm^3)	Cross-sectional area (mm^2)	Surface area (mm^2)
A	0.97 ± 0.07	26.45 ± 6.82	5.30 ± 0.29	93.77 ± 3.42
B	1.60 ± 0.14	50.08 ± 7.84	8.11 ± 0.51	111.89 ± 6.06
C	2.75 ± 0.14	105.77 ± 11.34	14.65 ± 0.59	132.37 ± 4.69

Values are mean $\pm$ standard deviation (S.D.).

plate speed was increased to 1045 rpm until liquid addition was completed. The frictional base plate was rotated for an additional 20 min at 520 rpm for tumbling before drying was carried out. The inlet temperature was then increased to 60 °C and the wall of the inner chamber was lifted for the fluidization and drying of spheroids until a constant exhaust air temperature was attained. For each of the three frictional base plates, five processing runs were carried out.

2.2.3. Size analysis

The percentages of yield, lumps and fines were calculated based on the total weight of starting material. Yield referred to the total amount of spheronized product recovered after the processing run. The fraction remaining on the sieve with aperture size of 2.8 mm, defined as lumps, was removed from the yield before the product was sub-divided by a riffler (PT, Retsch, Germany). A nest of sieves (Endecotts, UK) of aperture sizes giving a $\sqrt{2}$ progression within the size range of 0.25–2.8 mm was used to separate a weighed amount of spheroids of about 120 g into various size fractions. A sieve shaker (VS1000, Retsch, Germany) vibrating at 1 mm amplitude for 15 min was used for separating the spheroids into the various size fractions. The mass median diameter and span were employed to characterize the spheroid mean size and size distribution. The mass median diameter of the spheroids is the spheroid diameter at the 50% mark on the respective cumulative percent oversize plot. The span of spheroid size distribution is calculated as the ratio of the difference between the spheroids diameter at the 90% and at the 10% to the spheroids diameter at the 50%.

The fines fraction was the product fraction that passed through the 0.425 mm aperture size sieve. The modal class fraction referred to the size fraction obtained from sieving with the highest weight of spheroids.

2.2.4. Image analysis

At least 50 spheroids from each batch were randomly selected from the modal class fraction obtained from size analysis by sieving for image analysis. For each plate type, a total of five batches were tested. The image analyzer (PC Image 2.2, Foster Findlay Associates, UK) consisted of a computer system connected to a video camera (SSC-M370CE, Sony, Japan) mounted on a stereomicroscope (SZH, Olympus, Japan). The average projected area (A) and perimeter (P) of the spheroids were determined from the digitized images of the spheroids. A shape factor e_R which takes into consideration both deviation of shape from sphericity and surface irregularities was introduced by Podczeck and Newton (1994, 1995). A value for the shape factor below 0.7 describes a deviation from a perfect circular shape or surface irregularity but values above 0.6 can be considered to be satisfactory.

$$e_R = \frac{2\pi}{P}\frac{r_e}{f} - \sqrt{1 - \left(\frac{b}{l}\right)^2}$$

$$f = 1.008 - 0.231\left(1 - \frac{b}{l}\right)$$

where r_e is a mean radius determined from all the radii measured from each of the boundary points to the center of the object. The values of b and l are the length and the breadth of the two-dimensional particle outline, respectively. The value f is

a correction factor (Podczeck and Newton, 1995). The length is the maximum chord length of the object regardless of orientation. Firstly, the center of the area is found, then the furthest point on the object boundary from this center is determined. After that, the furthest boundary point from this point is found. Breadth is the projection of the object onto an axis perpendicular to the length. Circularity (C) values emphasize the spherical shape of spheroids (Vertommen et al., 1997). A value of unity describes a perfect circle.

$$C = \frac{4\pi A}{P^2}$$

2.2.5. Bulk and tapped densities

Spheroids were poured gently through a glass funnel into a graduated cylinder cut exactly to 100 ml with an inner diameter of 28 mm. Excess spheroids were removed using a spatula and the weight of the cylinder with spheroids was determined after testing. Weight of the spheroids required for filling the cylinder was calculated. The cylinder was then tapped for 600 times and the volume of spheroids was noted. Further tapping of 400 times was carried out to ensure the spheroids were tapped to a constant volume in tap density tester (STAV 2003, Stampfvolumeter, JEL Engelsmann, Germany). Bulk density (ρ_b) was calculated as the quotient of the weight of the spheroids and the volume of the cylinder used. Tapped density (ρ_t) was calculated as the quotient of the weight of the spheroids and its final volume after tapping. Hausner ratio (H_R) and Carr index (I_C) were calculated according to the two equations below:

$$H_R = \frac{\rho_t}{\rho_b}$$

$$I_C = \frac{\rho_t - \rho_b}{\rho_t}$$

2.2.6. Friability

An accurately weighed amount of spheroids, of about 10 g, taken from the modal class fraction of products was placed in a friabilator (TA20, Erweka®, Germany) and tumbled for 200 revolutions at 25 rpm. Twelve steel balls (diameter 6 mm, weighing 0.884 g each) were used as attrition agents. After friability testing, the spheroids were sieved through a series of sieves. The weight loss (%F) after friability testing was calculated as:

$$\%F = \frac{\mathrm{Wi} - \mathrm{Wr}}{\mathrm{Wi}} \times 100\%$$

where Wi was the initial weight of spheroids before friability testing, and Wr was the weight of spheroids retained above the sieve with 0.25 mm aperture size after friability testing.

3. Results and discussion

3.1. Characteristics of the studs on the frictional base plates

It can be seen from Table 1 that stud height, volume, cross-sectional area and surface area all followed an increasing trend going from plate A to C. For all four parameters, the differences observed between the three plates were significant analysis of variance (ANOVA, $P < 0.001$). From Table 2, stud height, volume and cross-sectional area of the studs were observed to be linearly related to each other. Significant positive Pearson correlation coefficient values were obtained (Pearson correlation, $P < 0.05$). The height at the tallest part of the stud and stud volume were directly measured from the studs while the cross-sectional area was calculated based on the width and height at the tallest part of the stud (Fig. 1). These three parameters had significant correlation with each other as they were all derived with reference to the stud height. Hence, stud height can be used to represent the other two parameters

Table 2
Correlation relationships of the various studs properties

	Standard characteristics of studs		
	Height	Volume	Cross-sectional area
Volume	1.000[a]	–	–
Cross-sectional area	0.998[a]	1.000[a]	–
Surface area	0.991	0.987	0.981

[a] Correlation is significant at the 0.05 level.

for plotting the relationships between spheroid properties and stud parameters. Stud surface area also showed an increasing trend with increasing stud height, volume and cross-sectional area. However, the Pearson correlation coefficient values ($P < 0.05$) between stud surface area and these other three studs parameters were not significant. A reason for this could be that stud surface area was not linearly related to the stud height.

3.2. Loading

From preliminary investigations, it was found that the load of powder mixture that could be used for the three different plates was influenced by the plate chosen, that is, the stud property (Liew et al., 2000b). During the liquid addition phase, the moistening liquid wets the powder particles and the starting material moves in a tumbling rope-like motion on the rotating frictional base plate under the influence of the combined action of centrifugal and kinetic forces, gravity and gap air. It was found the powder mass could not move freely if excessive starting material was loaded onto the rotating frictional base plate. Overloading resulted in only the bottom layer of starting material on the frictional base plate moved in a tumbling rope-like motion while the upper layer of powder remained relatively stationary. Under such circumstances, the continued addition of moistening liquid caused over-wetting of the powder mix in the vicinity of the spray nozzle. Lumps were formed and the powder mix may not be transformed from a powdery state into a moist granular mass suitable for spheroid production. Loads of 600, 800 and 1000 g were used on the three frictional base plates. With similar formulation and processing conditions, it was observed that plate A, with the shortest studs, was only effective for a 600 g load of starting material but not a higher load of 800 g. Plate B, with studs of medium height, was effective for both the 600 and 800 g loads. At the conditions used, spheroid production with 1000 g load on plate B was not as stable as with the lower loads of 600 and 800 g. Plate C, with the tallest studs, was found to be able to be effective over the widest load range among the three plates. It was effective for the whole range of loads tested in the study from 600 to 1000 g. Hence, for comparing the three frictional base plates, a 600 g load of starting material was chosen as this load could be supported by all three plates.

3.3. Adhesion and yield

Due to the lining of PTFE tape on the wall of inner chamber, there was very little adhesion on the wall throughout the processing run. After the completion of each run, the spheroids was discharged carefully from the inner chamber and collected, leaving the base plate for examination to show evidence of material adhesion. From Table 3, visual observations showed that plate A, with the shortest studs, had very low level of moist powder adhesion. Only a thin powder film layer was found on the surface of plate A. Plate B, with studs of medium height, had more material adhesion than plate A but less adhesion compared with plate C. The amount of material adhesion on the studs of plate B consisted mainly of some moist material lodged adjacent to the heads of the teardrop-shaped studs. Plate C, with the tallest studs, had comparatively the heaviest amount of material adhesion. It could be observed that the adhered mass comprised not only moist powder but also some spheroids. More adhesion was observed in the valley area next to the stud head, where stud height and stud width were at their tallest and broadest dimensions, respectively. With an increase in stud height, the depth of the valley at the stud head increased correspondingly. Hence, this led to a greater tendency for the entrapment of moist material at the valley areas adjacent to the stud heads during the liquid addition stage of the rotary spheronization run. Moist spheroids formed may also be caught onto the adhered moist powder layer as they tumbled on the rotating frictional base plate thereby increasing the amount of material adhesion on the plate surface.

In previous studies, studs on the frictional base plates used were symmetrical (Liew et al., 1998, 2000a; Holm, 1996; Wan et al., 1994, 1995). Hence, moist material had a tendency to be trapped in the valley encircling the whole stud. In

Table 3
Physical characteristics of spheroids produced using the three different frictional base plates

Plate	Observations	Bulk density (g/ml)	Tapped density (g/ml)	Hauser ratio	Carr index	Friability (%)
A	Slight adhesion, in the form of a thin film layer of powder	0.831 ± 0.008	0.862 ± 0.004	1.037 ± 0.007	3.60 ± 0.71	0.72 ± 0.37
B	More adhesion than plate A but less adhesion than plate C. Only some wetted powder was caught around the stud heads	0.841 ± 0.015	0.870 ± 0.013	1.035 ± 0.006	3.34 ± 0.55	0.54 ± 0.22
C	Heavy adhesion on plate and some spheroids were found stuck onto the adhered material at the areas around the stud heads	0.821 ± 0.023	0.855 ± 0.018	1.041 ± 0.008	3.95 ± 0.74	0.33 ± 0.14

Values are mean $\pm$ S.D.

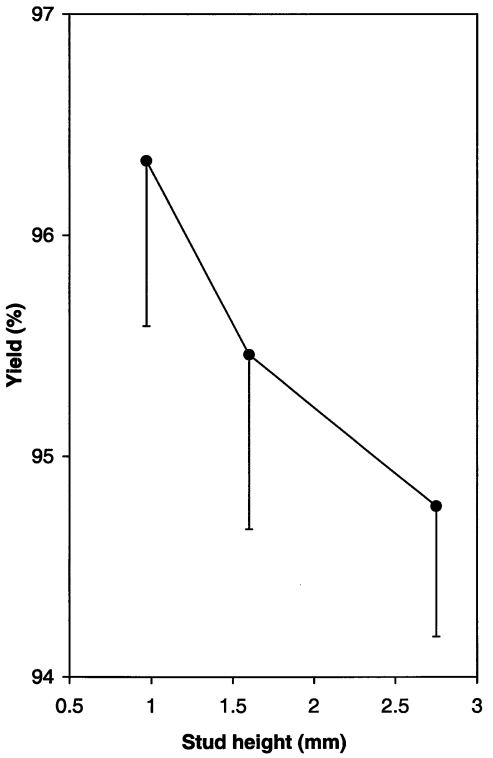

Fig. 2. Yield of spheroids prepared using plates with different stud height.

this present study, with a broad head tapering to a tail, the height and width of the teardrop studs decreased from the stud head towards the tail end. The rotation of the frictional base plate was in a clockwise direction following the streamline nature of the studs, from the tail end moving forward towards the head of the stud. Due to their asymmetrical, streamline and tapering nature, adhesion on these teardrop studs can be reduced by limiting adhesion to the valley area at the stud head where stud height and width were at their largest dimensions as observed in this study.

From Fig. 2, spheroid yield decreased with an increase in the height of the studs on the rotating frictional base plate. There was significant difference between yields obtained with plate A and with plate C (ANOVA, $P < 0.05$). The decrease in the yield could be attributed to the material adhesion on the rotating frictional base plate. With a fixed load of starting material, greater adhesion corresponded to a lower spheroid yield. This effect became more critical with smaller loads of starting material.

3.4. Size, size distribution, lumps and fines

In the production of spheroids by rotary spheronization, it is ideal for the spheroid batch to have a high yield, the desired mean size and a narrow size distribution. Span values reflected the homogeneity of the spheroid batch. A smaller value indicated a narrower and tighter spheroid size distribution with a lower 'within batch' variability. Oversize particles were undesirable and should be minimized as the presence of such lumps in the spheroid yield was often an indication that the single step agglomeration–spheronization process proceeded in a less stable and unpredictable manner. The formulation and processing conditions used in this study were chosen such that spheroids with the desired mean size, around 1 mm, could be produced for all three frictional base plates.

When the three plates were used for spheroid production, trends of increasing mass median diameter of spheroids and decreasing span were observed with increasing stud height and stud surface area (Fig. 3). Differences between the mass median diameter of spheroids produced by plate C, with the tallest studs, and those of spheroids formed with the other two plates were found to be significant (ANOVA, $P < 0.05$). For span, significant differences existed between spheroids produced by plate A, with the shortest studs, and spheroids produced using the other two plates (ANOVA, $P < 0.05$). The amount of lumps in the product obtained from plate A was significantly larger (ANOVA, $P < 0.05$) than the amounts obtained with the other two plates (Fig. 4). The fines fraction from plate A was also greater than those from the other two plates. There was a positive and significant correlation (Pearson correlation, $P < 0.05$) between the mass median diameter of the resultant spheroids and the height, volume and cross-sectional area of studs.

In rotary processing, spheroids were formed directly from a powder mix by what may be

described as an agglomeration–spheronization process. With the addition of moistening liquid, powder particles formed aggregates. The moist aggregates, on random collision or adhesion with one another, undergo coalescence, fusing to form larger units. Spheroids were subsequently formed during the liquid addition phase and continued to grow to an optimum size after the complete addition of the moistening liquid. Agglomerate surface moisture may be increased by liquid addition and/or by the squeezing out of moisture from the agglomerate interior during densification when the agglomerates traveled in a tumbling rope-like motion on the rotating frictional base plate. For single step spheroid production by rotary spheronization, protuberances on plate surface were necessary to increase the frictional area between spheronizing material and plate so as to supply sufficient shear and impact to the powder mass to effect material movement for agglomeration and spheronization.

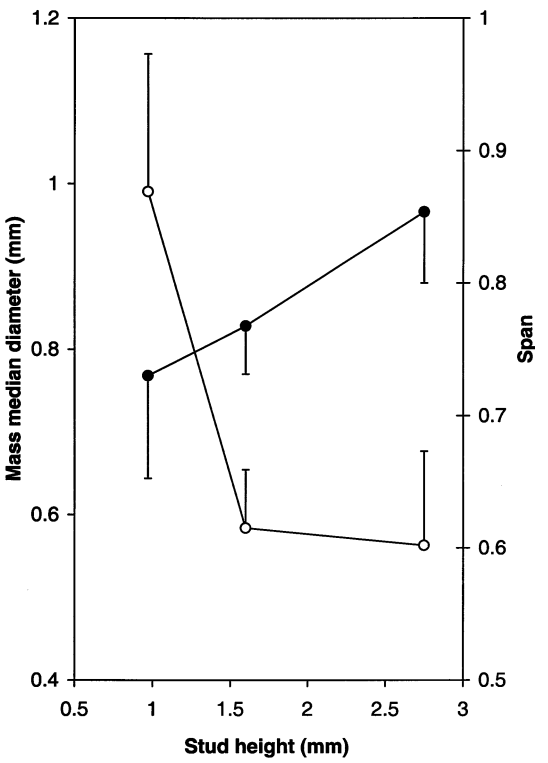

Fig. 3. Mass median diameter (●) and span (○) of spheroids prepared using plates with different stud height.

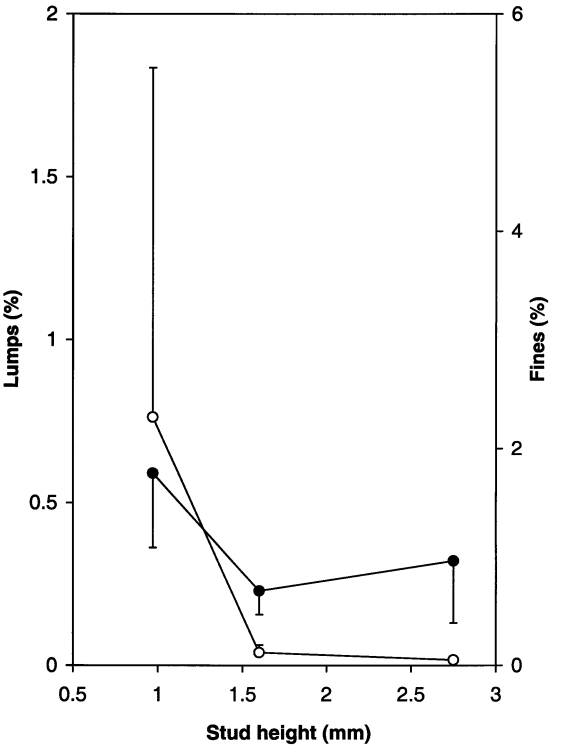

Fig. 4. Lumps (●) and fines (○) fractions obtained using plates with different stud height.

Following an increase in stud height, the increase in surface area increased the frictional contact area between the plate and the spheronizing material. With taller studs, the increased elevation in the vertical plane also resulted in material being propelled up a slope with a steeper gradient. The material moving on the rotating base plate was also confronted by a larger overall vertical area and volume as indicated by the larger stud cross-sectional area and volume. When the plates were rotated at the same speed, the powder mass on the base plate with taller studs, therefore, experienced greater shearing and impact per unit time. The higher forces generated intensified the mixing action of the moistened powder mass. This improved the distribution of moistening liquid to the powder mass. A more homogeneous liquid distribution was obtained with a decrease in the tendency for overwetting and a reduction in the occurrence of lumps in the spheronized product as can be observed from comparing plate A with

plates B and C (Fig. 4). Consequently, the size distribution of the spheroid batch was reduced by using plates with taller studs.

Besides more intensive mixing and improved liquid distribution, the enhanced material movement on the rotating frictional base plate increased the chances for moist agglomerates to collide with each other and with the chamber wall. The agglomerates could undergo greater deformation, densification and coalescence, leading to the formation of spheroids with comparatively larger mean size.

The greater shear and energy input also made it possible for plates with taller studs to be effective with a greater load for rotary spheronization. This has been shown previously where plate C, with the tallest studs, was found to be able to be used with higher load, compared with the other two plates with shorter studs.

3.5. Shape

Sphericity is also an important particle characterization parameter as the shape of particles can affect other properties such as flowability and coating performance. It can be seen from Fig. 5 that the e_R value increased from 0.477 to 0.609 and the circularity values increased from 0.891 to 0.940 when stud height increased from plate A to C. Nevertheless, for e_R and circularity, there were significant differences among all of the three plates (ANOVA, $P < 0.05$). A positive and significant correlation (Pearson correlation, $P < 0.05$) was observed between e_R and the height of stud on the plates. The shape factor e_R is sensitive to detect the difference of the shape of spheroids produced from three plates. The plate C with a taller stud can produce spheroids with acceptable sphericity because the value of e_R is bigger than 0.6. While the spheroids produced from the other two plates are not highly spherical due to the smaller e_R value. Although circularity used as a shape factor has some limitation, the values of circularity do show the same trend as that of e_R values.

In the production of spheroids, it is essential that spheroids undergo the tumbling rope-like movement in the rotary processor for an adequate period of time with sufficient consolidation forces. This rope-like movement removes irregularities or protrusions on the spheroid surface by mainly collisions between the forming spheroids on rotating frictional base plate surface and the chamber wall. Taller studs can produce higher impact forces to compact the wetted spheroid mass and enhanced the spheroid rounding process. The rolling motion of spheroids on the rotating frictional base plate and the inner wall supported the smoothening of spheroid surfaces. Longer tumbling time was also reported to have the same contribution to smoothening of spheroids (Wan et al., 1994).

3.6. Density and friability of spheroids

It has been reported that spheroids prepared in a rotary fluid bed have comparatively lower porosity and higher bulk density compared with agglomerates produced by the typical top-spray

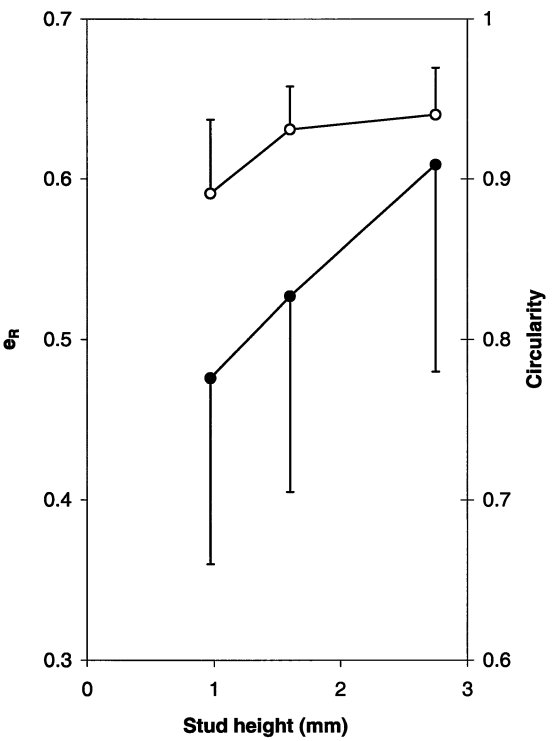

Fig. 5. Shape factor e_R (●) and circularity (○) of spheroids prepared using plates with different stud height.

granulated fluid bed process (Parikh et al., 1997). From the results presented in Table 3, it can be seen that all the bulk density values of the spheroids prepared with the three frictional base plates varied between 0.82 and 0.84 g/ml and the tapped density values between 0.86 and 0.87 g/ml. A high Hausner ratio indicates increased cohesion between particles and, therefore, poorer flow. The Hausner ratio values of the spheroid batches varied from 1.035 to 1.041, indicating good flow properties of the spheroids. Due to the high degree of sphericity, good flowability and narrow size distribution of spheroids, the weight variation of spheroid-packed capsules by volumetric measures is expected to be small.

Investigation on spheroid friability showed that there was minimal weight loss after friability testing as spheroids formed by rotary processing were spherical, dense and smooth with minimal protruding surfaces. Nevertheless, for percentage weight loss after friability testing, the values obtained for plate A and C were significantly different (ANOVA, $P < 0.05$). Spheroids produced with plate C were significantly less friable compared with those produced using plate A. Spheroid friability can also be used to give an indication of spheroid strength, with a lower friability reflecting greater spheroid strength. From these findings, it could be extrapolated that spheroids prepared with plate C, as compared with those produced using plate A, were densified to a greater extent, giving relatively stronger agglomerates.

3.7. Between batch variability

For single step spheroid production by rotary processing, it is essential to ensure that each run produces a high yield of spheroids with the desired mean size within a narrow size distribution. Besides 'within batch' variability, 'between batch' variability of the spheroid batches was investigated for process reproducibility of the three different base plates. For each plate, a larger deviation from the mean value of each spheroid parameter obtained from five spheroid batches would indicate a greater 'between batch' variability and, therefore, poorer process reproducibility. On the whole, among the three base plates, the largest 'between batch' variability for mass median diameter, span, lumps, fines and circularity was observed with plate A which had the shortest studs (Figs. 3–5). In particular, the deviations from the mean values of % lumps and % fines reduced markedly when stud height was increased from plate A to B and C (Fig. 4). For yield and e_R, all three plates had rather similar 'between batch' variability (Figs. 2 and 5). For mass median diameter and span of spheroids, the deviation for plate B was marginally smaller than for plate C (Fig. 3). For circularity, the deviation for plate C was marginally smaller than for plate B (Fig. 5). These findings implied that, in general, the spheroid production using plate A, with greater variability between batches, was comparatively less stable and less reproducible than spheroid production using plates B and C.

4. Conclusion

Differences in height, volume, cross-sectional area, surface area of studs on the three rotating frictional base plates influenced the magnitude of forces imparted by the rotating frictional base plate to the starting powder mass in the rotary spheronization process. Consequently, the resultant spheroids varied in spheroid properties such as size, size distribution, shape and friability. The forces set up by the base plate must be sufficient for promoting homogeneous liquid distribution, powder mass mixing and spheroid formation without excessive coalescence and uncontrollable growth while minimizing adhesion on the base plate. Plates B and C both gave spheroids with better 'within batch' spheroid characteristics than plate A. Plate B with studs of medium height was also demonstrated to give the best overall reproducibility in this study. A balance between good reproducibility and 'within batch' spheroid characteristics with minimal material adhesion could be achieved with plate B. Hence, under the similar formulation and processing conditions used in this study, plate B was concluded as the most suitable among three plates with teardrop studs of different heights. However, if higher loads are to be used, plate C may be more suitable as it was

shown to be able to support higher loads. When larger loads are used, the amount of material loss attributed to adhesion of moist material onto the rotating frictional base plate also becomes less critical as it accounts for a smaller percentage of the total load used for spheroid production.

References

Holm, P., 1996. Pelletization by granulation in a Roto-Processor RP-2. Part II: effects of process and product variables on agglomerates' shape and porosity. Pharm. Tech. Int. 8, 38–45.

Liew, C.V., Wan, L.S.C., Heng, P.W.S., 1998. Influence of polytetrafluoroethylene on spheroid production by rotary processing. S.T.P. Pharm. Sci. 8, 297–302.

Liew, C.V., Wan, L.S.C., Heng, P.W.S., 2000a. Role of base plate rotational speed in controlling spheroid size distribution and minimizing oversize particle formation during spheroid production by rotary processing. Drug Dev. Ind. Pharm. 26, 953–963.

Liew, C.V., Gu, L., Heng, P.W.S., 2000b. Influence of teardrop studs on frictional plate on spheroid quality in rotary processing. 10th International Pharmaceutical Technology Symposium—Development and Delivery Challenges of the Next Generation of Drugs, Turkey, pp. 195–196.

Parikh, D.M., Bonck, J.A., Mogavero, M., 1997. Batch fluid bed granulation. In: Parikh, D.M. (Ed.), Handbook of Pharmaceutical Granulation Technology. Marcel Dekker, Inc, New York, pp. 287–291.

Podczeck, F., Newton, J.M., 1994. A shape factor to characterize the quality of spheroids. J. Pharm. Pharmacol. 46, 82–85.

Podczeck, F., Newton, J.M., 1995. The evaluation of a three dimensional shape factor for the quantitative assessment of the sphericity and surface roughness of pellets. Int. J. Pharm. 124, 253–259.

Vertommen, J., Rombaut, P., Kinget, R., 1997. Shape and surface smoothness of pellets made in a rotary processor. Int. J. Pharm. 146, 21–29.

Wan, L.S.C., Heng, P.W.S., Liew, C.V., 1994. The role of moisture and gap air pressure in the formation of spherical granules by rotary processing. Drug Dev. Ind. Pharm. 20, 2551–2561.

Wan, L.S.C., Heng, P.W.S., Liew, C.V., 1995. The influence of liquid spray rate and atomising pressure on the size of spray droplets and spheroids. Int. J. Pharm. 118, 213–219.